

Supporting information

Self-assembled GaN quantum wires on GaN/AlN nanowire templates

Jordi Arbiol, *^a Cesar Magen,^{b,c} Pascal Becker,^d Gwénoél Jacopin,^e Alexej Chernikov,^f Sören Schäfer,^f Florian Furtmayr,^{d,g} Maria Tchernycheva,^e Lorenzo Rigutti,^{e,i} Jörg Teubert,^d Sangam Chatterjee,^f Joan R. Morante^h and Martin Eickhoff,*^d

^a *Institució Catalana de Recerca i Estudis Avançats (ICREA) and Institut de Ciència de Materials de Barcelona, ICMAB-CSIC, Campus de la UAB, E-08193 Bellaterra, CAT, Spain E-mail: arbiol@icrea.cat*

^b *Laboratorio de Microscopías Avanzadas, Instituto de Nanociencia de Aragon-ARAID, Universidad de Zaragoza, 50018 Zaragoza, Spain*

^c *Departamento de Física de la Materia Condensada, Universidad de Zaragoza, 50009 Zaragoza, Spain*

^d *I. Physikalisches Institut, Justus-Liebig-Universität Gießen, Heinrich-Buff-Ring 16, DE-35392 Gießen, Germany E-mail: eickhoff@physik.uni-giessen.de*

^e *Institut d'Electronique Fondamentale, University of Paris Sud XI, UMR 8622 CNRS, 91405 Orsay, France*

^f *Faculty of Physics and Materials Science Center, Philipps Universität Marburg, Renthof 5, DE-35032 Marburg, Germany*

^g *Walter Schottky Institut, Technische Universität München, Am Coulombwall 4, DE-85748 Garching, Germany*

^h *Catalonia Institute for Energy Research, IREC. 08930 Sant Adrià del Besòs, Spain and Department d'Electrònica, Universitat de Barcelona, 08028 Barcelona, Spain*

ⁱ *present address: Groupe de Physique des Matériaux, UMR CNRS 6634, University of Rouen, 76801 St Etienne du Rouvray, France*

* authors to whom correspondence should be addressed (arbiol@icrea.cat, eickhoff@physik.uni-giessen.de)

CONTENTS Page

S1. Electron Beam damage and 3D QWRs view (Figure S1)	2
S2. GaN/AlN heterostructures Plan View (Figure S2)	3
S3. 3D view of the QWRs grown on the NW edges (sample F) (Figure S3)	3
S4. Diameter modulation: Single ML QWR (sample F) (Figure S4)	4
S5. Strain analysis and direct Polarity determination (sample F) (Figure S5).....	5
S6. Beam damage on sample D (Figure S6)	6
S7. 3D atomic models for different diameter QWRs (Figure S7)	7
S8. Material Parameters used for the Simulations (Table S1)	8
S9. Simulation of the influence of the AlN capping layer on the QWR transition energies (Figure S8).....	9
References	10

S1. Electron Beam damage and 3D QWRs view

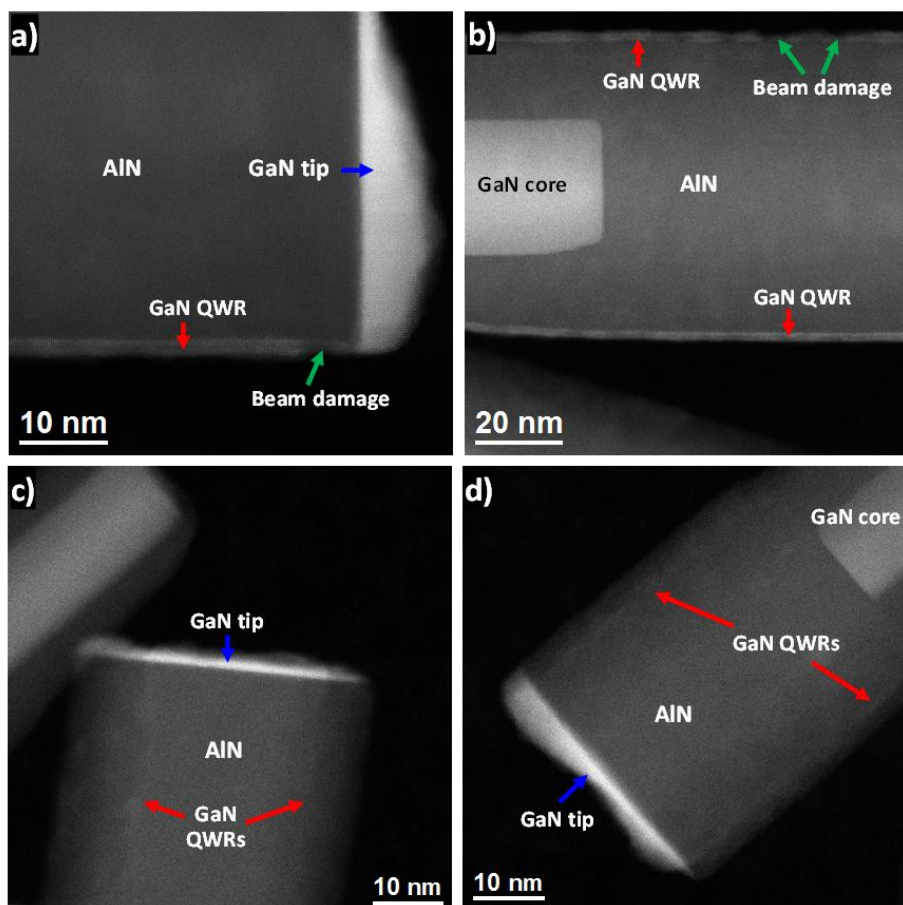


Fig. S1 a) HAADF STEM view showing one of the NW heterostructures from *sample A*. b) HAADF STEM aberration corrected image showing a couple of QWRs with induced e-beam damage after a few minutes of exposure. c) Z-contrast detail of the GaN QWRs when rotating the nanowire heterostructure. d) same as c) in another nanowire. Out of the [11-20] zone axis the QWRs are not easily focused and appear diffuse on the image (also affected by beam damage).

In sample A no protective AlN cap layer has been deposited on the QWRs, which affects their stability under the microscope electron beam (300 keV). Micrographs shown in the manuscript body (**Figure 1**) were obtained during the first seconds of exposure. After less than a minute, the QWRs are severely damaged by the electron beam, start to decompose and become amorphous (**Figures S1 a)** and **b)**).

Figures S1.c) and **d)** show the NW rotated out of the [11-20] zone axis in order to avoid the QWR overlapping and give a 3D-view sense. Notice that QWRs are diffuse due to the small depth of focus of the HAADF-STEM technique as well as the introduced beam damage. The beam damage was drastically reduced when depositing an AlN shell (*Samples E* and *F*).

S2. GaN/AlN heterostructures Plan View.

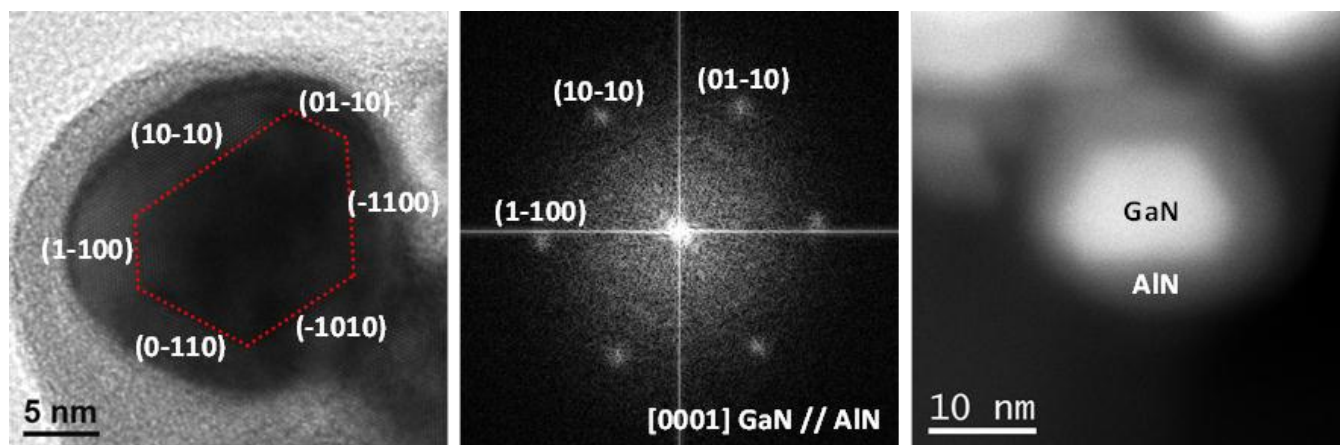


Fig. S2 (left) HRTEM cross-section of a GaN NW surrounded by the AlN shell. The GaN core (red dotted sidewalls) forms a hexagonal prism section with $\{10-10\}$ planes (m planes) as lateral facets. The surrounding AlN shell is more cylindrical with rounded facets. (middle) Corresponding selected area electron diffraction (SAED) pattern, proving that the sidewalls are m planes. (right) HAADF STEM image.

The GaN core forms a hexagonal prism section with $\{1-100\}$ planes (m -planes) as lateral facets, as observed in Fig. S2. This result is in good agreement with the profile obtained in Figure 2f) of the manuscript body and also with the results of previous works.^[1]

S3. 3D view of the QWRs grown on the NW edges (sample F).

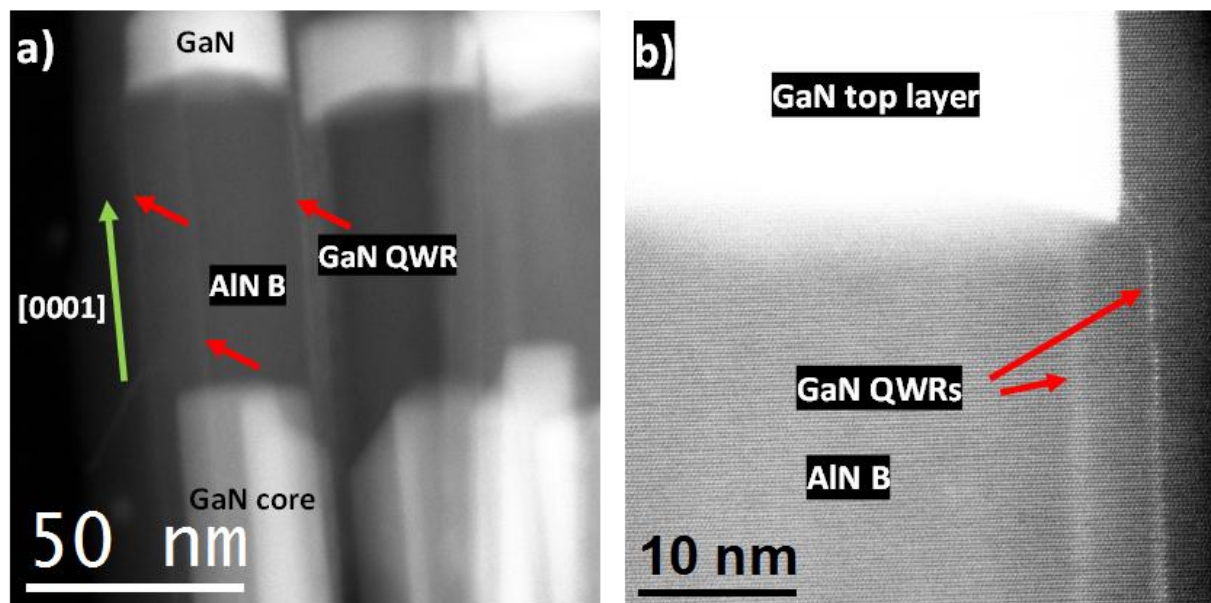


Fig. S3 a) HAADF-STEM general view of *sample F*, i.e. NW heterostructures containing the QWRs (pointed by red arrows) and an AlN cap layer. The NWs have been rotated slightly out of the $[11-20]$ zone axis in order to give a 3D view impression. In this way more QWRs can be visualized at the same time avoiding QWRs projected overlapping. b) Magnified detail obtained at atomic resolution by means of aberration corrected HAADF-STEM. Resolution is not optimized due to the off-axis imaging.

In **Figure 2** of the manuscript body we show the QWRs along the [11-20] axis projection. For a high quality atomic resolution image it is necessary to observe the nanostructures along one of the high-symmetry (low-index) zone axes. However, during imaging of that type, the QWR structures deposited on the NW edges can be overlapped on the STEM projection. Notice that due to the small HAADF-STEM depth of focus (5-10 nm), the atomic resolution is only obtained on one of the QWRs, however visualization of the ones underneath (those overlapped) is hindered. In order to distinguish the different edge QWRs, we have slightly rotated the NW out of the [11-20] zone axis in order to avoid overlapping and give a 3-dimensional (3D) sense of the nanostructure. In **Figure S3**, we present this 3D effect, allowing visualizing some of the QWRs otherwise overlapped in **Figure 2** of the text body. Also due to the small depth of focus of the HAADF-STEM,^[2] the front QWR is observed as a sharp feature (on focus) while the one beneath is out of focus.

S4. Diameter modulation: Single ML QWR (sample F).

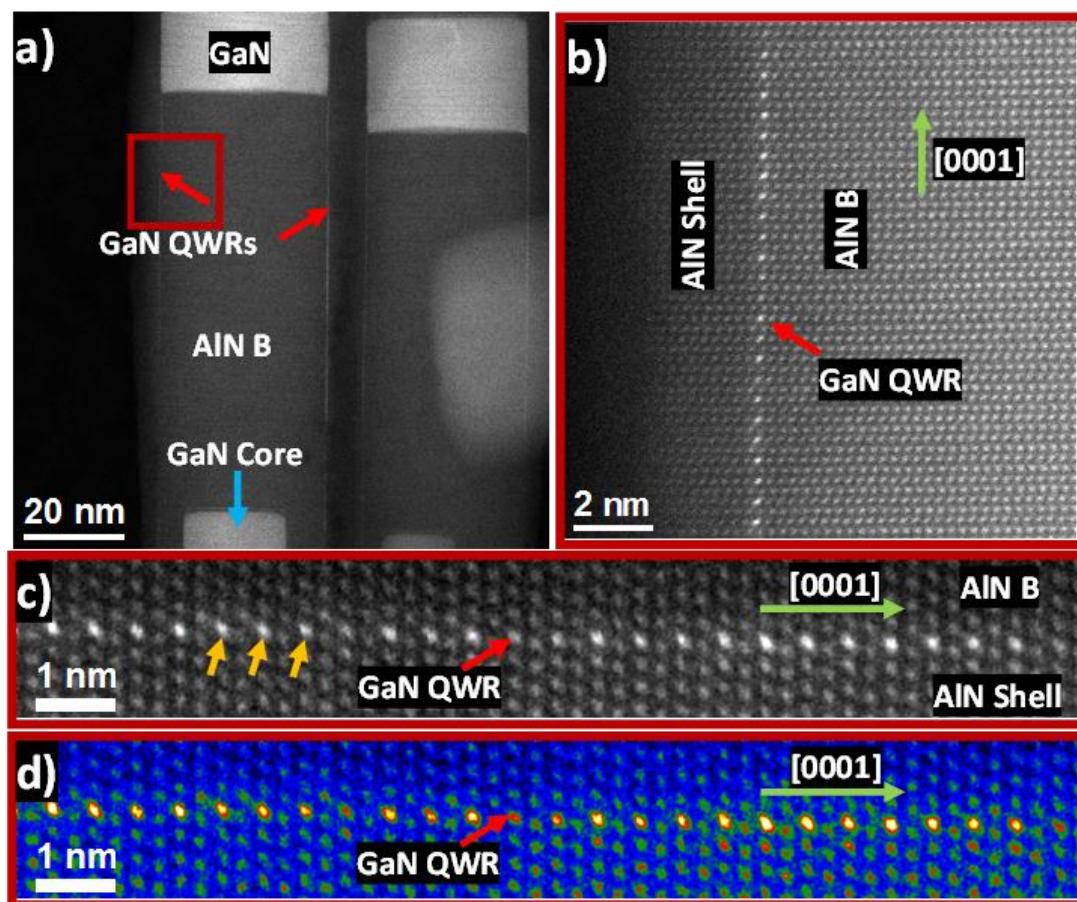


Fig. S4 a) General HAADF STEM view showing the lateral QWRs (pointed with red arrows) of the NW heterostructure from *sample F*. b) Atomic resolution HAADF STEM aberration corrected image showing the discrete GaN monoatomic QWR (single ML). c) Z-contrast magnified detail of the GaN monoatomic QWRs, brightest atomic columns correspond to the ones containing Ga atoms. d) Same as c) but applying false color to enhance the contrast.

In **Figure S4** we demonstrate the achievement of a single ML QWR. This wire has 1 single GaN plane section, implying the perfect 1-dimensional distribution. Although there is no physical volume for quantum effects, this achievement remarks on one side the lower limits for GaN deposition on the AlN shell edges, as well as the power of the applied detection technique (atomic resolution aberration corrected HAADF-STEM). The visualization of these single Ga atoms is possible due to the high difference in atomic number between Ga ($Z = 31$) and Al ($Z = 13$), using Z-contrast imaging (intensity being proportional to Z^2).

S5. Strain analysis and direct Polarity determination (sample F).

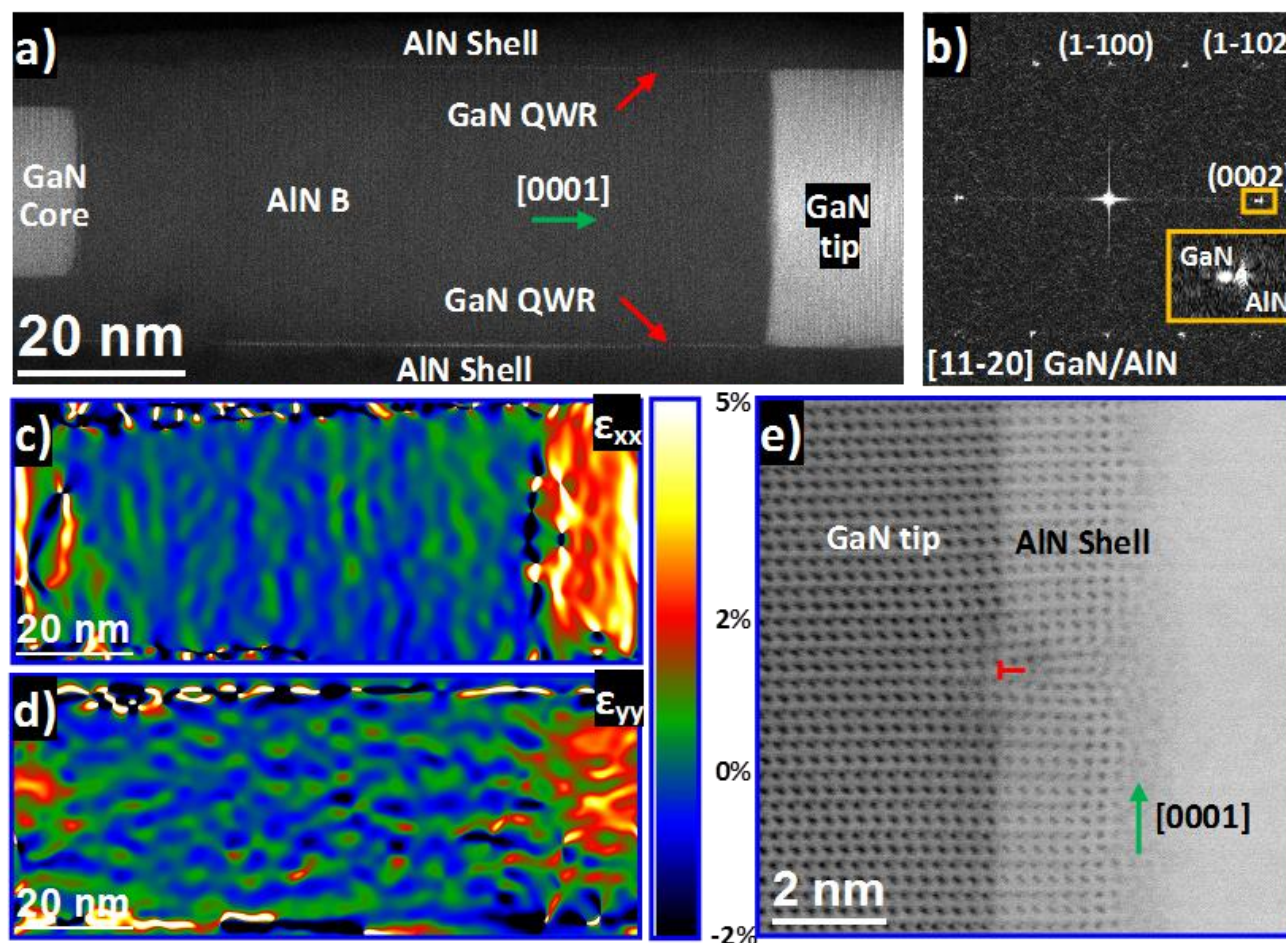


Fig. S5 a) Aberration corrected HAADF STEM detail of one of the QWRs on NW templates in *sample F* (the lateral QWRs are pointed with red arrows). B) Power spectrum obtained on the same image showing the partial relaxation of the top GaN layer versus the AlN barrier and shell. c) ϵ_{xx} strain map showing the partial relaxation of the GaN and AlN. d) ϵ_{yy} strain map showing also the partial relaxation on the y axis. e) Aberration corrected atomic resolution ABF STEM image showing the N-polarization in both the GaN and the AlN shell.

In **Figure S5** we have performed a strain analysis of the sample. From HAADF STEM atomic resolution images we have found that AlN is partially relaxed when growing on top on the GaN core (see Figures S5c and 5d for ϵ_{xx} and ϵ_{yy} strain components). For a full relaxation, the GaN and AlN (0002) planes (x-axis; ϵ_{xx} strain component **Fig. S5c**) should have a mismatch of around 4.4% (bulk), while our calculations show a mean mismatch of 2.9% which gradually increases to the GaN tip up to

4%. In the case of the (1-100) planes (y-axis; ϵ_{yy} strain component **Fig. S5d**), a mismatch of 3.2% should be expected for full relaxation, however we find an ϵ_{yy} value of 2.2% with a maximum of 2.5%.

In **Figure S5e** we show, by means of the newly developed aberration corrected atomic resolution annular bright field (ABF) STEM imaging, the N-face polarity in both the GaN and the AlN shell, as reported elsewhere.^[3] In addition, we show a clear misfit dislocation, which allows the observed partial relaxation of the heterostructure.

S6. Beam damage on sample D.

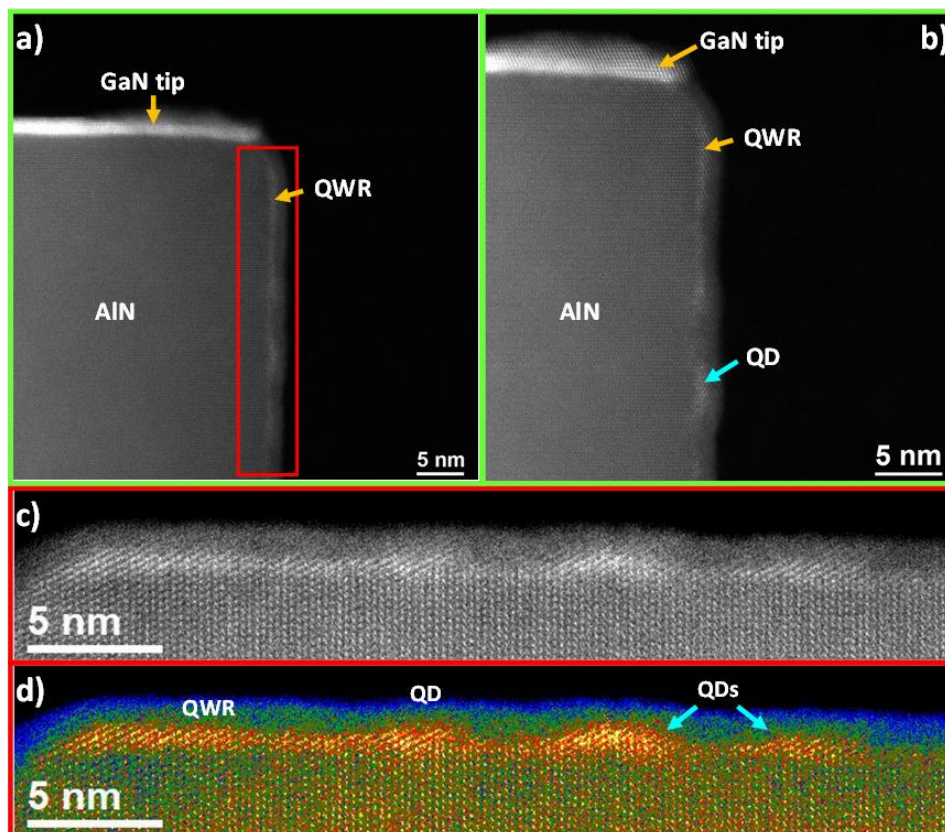


Fig. S6 a-d) Aberration corrected HAADF STEM detail of one of the QWRs NW templates in sample D.

In atomic resolution HAADF STEM images we can appreciate a continuous GaN QWR with a diameter of just 2 {1-100} projected monolayers (also equivalent to 2 {11-20} MLs), and from time to time, the formation of a confined 4 {1-100} projected monolayers quantum dot (QD)-like structures. Due to the beam damage the QWR has been partially evaporated creating discontinuities, allowing at the same time the formation of quantum dot (QD) structures and strain relaxation.

S7. 3D atomic models for different diameter QWRs

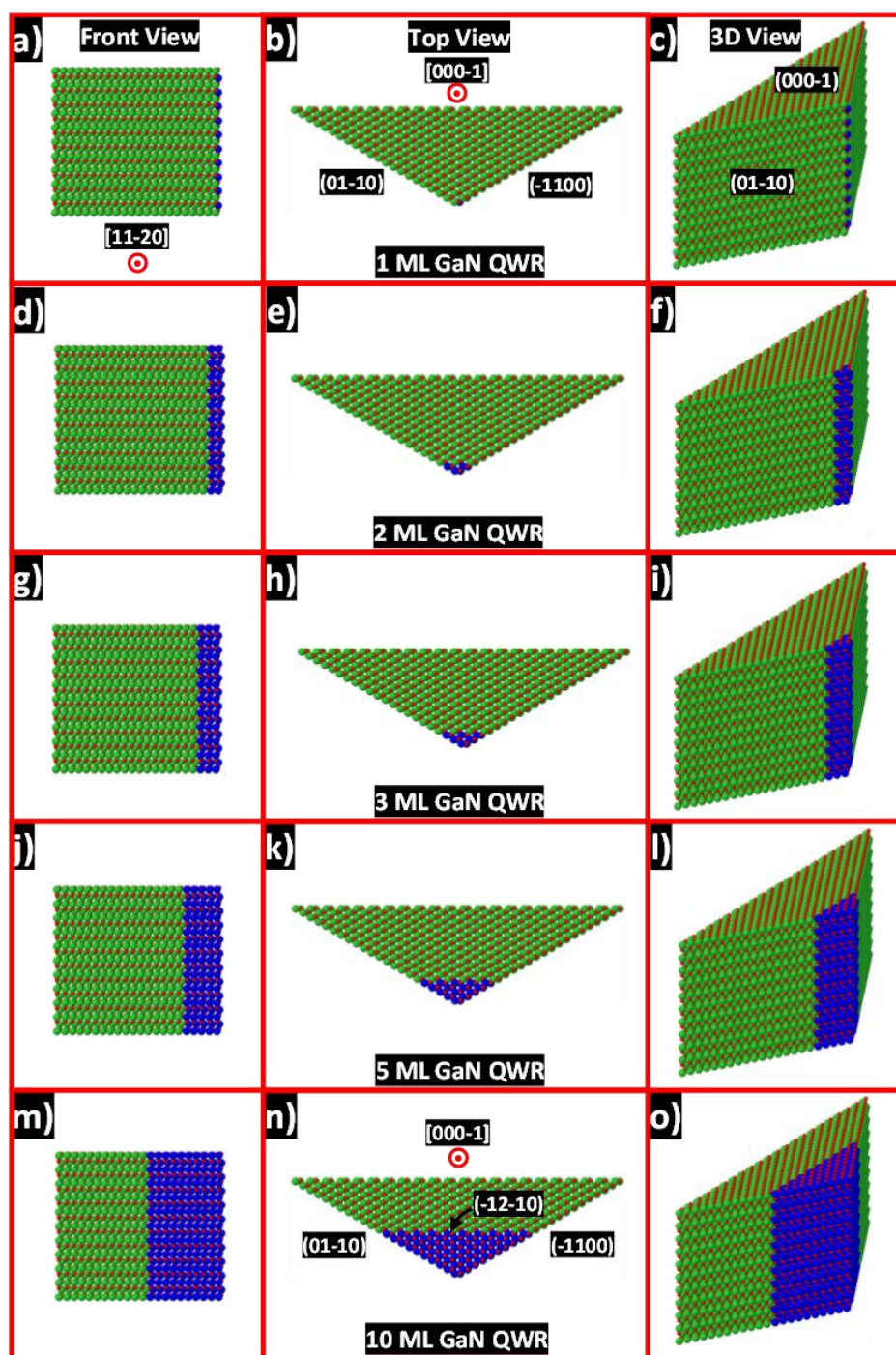


Fig. S7 Detailed 3D atomic models for different diameter QWRs. Every row corresponds to a different QWR diameter: (a-c) 1 GaN monolayer (ML), (d-f) 2 ML, (g-i) 3 ML, (j-l) 5 ML and finally (m-o) 10 ML. The first column displays the visualization in a front view projection (along the $[-1010]$ axis), equivalent to the one observed in the HAADF STEM images. Middle column correspond to the top view, along the growth NW growth axis or $[000-1]$. Finally the third column corresponds to a 3D perspective view. See also the following link for the corresponding animated 3D atomic simulations: <http://www.icmab.cat/gaen/research/165>

Attending to the projections observed on the HAADF STEM images, we could perfectly assume that the QWRs grow on the edges of the $\{1-100\}$ (m-planes) AlN hexagonally faceted NWs, when these edges

are slightly truncated, presenting {11-20} facets (a-planes). This is in good agreement with the projections observed experimentally, as well as with the theory and previous reports.^[1] The QWRs would have a triangular prismatic morphology, with external facets corresponding to {1-100} (m-planes), and epitaxed to the NW AlN shell through a {11-20} facet (a-planes), corresponding to the truncated edges.

S8. Material Parameters used for the Simulations.

Parameter	GaN	AlN
a [nm]	0.3189	0.3112
c [nm]	0.5185	0.4982
m* perpendicular	0.202	0.30
m* parallel	0.206	0.32
$E_c^{*})$	2.7997	4.7245
$E_{v,1}^{*})$	-0.717	-1.576
C_{11}	390	396
C_{12}	145	137
C_{13}	106	108
C_{33}	398	373
C_{44}	105	116
e_{33} [C/m ²]	1.27	1.79
e_{31} [C/m ²]	-0.35	-0.50
e_{15} [C/m ²]	-0.30	-0.48
Spontaneous polarization [C/m ²]	-0.0340	-0.0900
a_1 [eV]	-4.9	-3.4
a_2 [eV]	-11.3	-11.8
D_1 [eV]	-3.7	-17.1
D_2 [eV]	4.5	7.9
D_3 [eV]	8.2	8.8
D_4 [eV]	-4.1	-3.9
D_5 [eV]	-4.0	-3.4
D_6 [eV]	-5.1	-3.4

^{*)} with respect to the standard hydrogen electrode

Table S1 Material parameters for GaN and AlN used in the nextnano³-simulations according to ref.^[4]

S9. Simulation of the influence of the AlN capping layer on the QWR transition energies

Based on the geometric model for QWR growth described in the main text and schematically depicted in the insert of **Figure 6b** we have calculated the effect of the presence of an AlN capping layer on the QWR transition energies. In particular the effect of the resulting hydrostatic strain exerted by the three-dimensional embedment of the GaN QWR in the AlN matrix was taken into account.

In **Figure S.8** the resulting transition energies are displayed as a function of the thickness of the surrounding AlN material for a QWR diameter of 1.84 nm (triangle base length of 20 monolayers). Due to hydrostatic compression the QWR transition energies increase with increasing AlN shell thickness and saturate above a thickness of approximately 10 nm. From these results the blue shift due to the presence of the AlN capping layer was determined to approximately 90 meV.

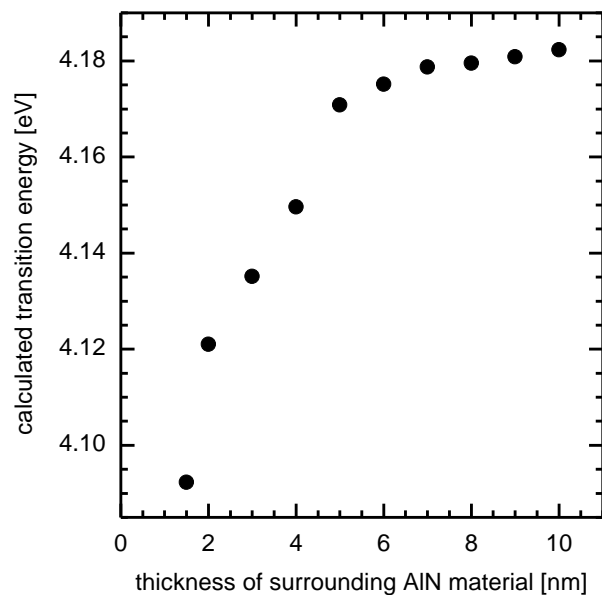


Fig. S8 Dependence of the calculated QWR transition energies on the thickness of the surrounding AlN material using the geometric model for QWR growth described in the text and schematically depicted in the insert of **Figure 6b** for a QWR diameter of 1.84 nm.

References

- [1] F. Furtmayr, J. Teubert, P. Becker, S. Conesa-Boj, J. R. Morante, J. Arbiol, A. Chernikov, S. Schäfer, S. Chatterjee and M. Eickhoff, *Phys. Rev. B*, 2011, **84**, 205303.
- [2] E. Uccelli, J. Arbiol, C. Magen, P. Krogstrup, E. Russo-Averchi, M. Heiss, G. Mugny, F. Morier-Genoud, J. Nygard, J.R. Morante and A.F.I. Morral, *Nano Lett.*, 2011, **11**, 3827
- [3] M. de la Mata, C. Magen, J. Gazquez, M.I.B. Utama, M. Heiss, S. Lopatin, F. Furtmayr, C.J. Fernández-Rojas, B. Peng, J.R. Morante, R. Rurali, M. Eickhoff, A. Fontcuberta i Morral, Q. Xiong and J. Arbiol, *Nano Letters*, 2012, **12**, 2579.
- [4] I. Vurgaftman and J. R. Meyer, *J. Appl. Phys.*, 2003, **94**, 3675.